Defect and Diffusion Forum Vols. 273-276 (2008) pp 431-444
online at http://www.scientific.net

Online available since 2008/Feb/11

Visualization of the Vacancy-Wind Effect Occurring in Chemical Diffusion and Ionic Conductivity in Solids*

I.V. Belova[1,a] and G.E. Murch[1,b]
[1]Diffusion in Solids Group,
Centre for Geotechnical and Materials Modelling,
School of Engineering
The University of Newcastle, Callaghan, NSW 2308, Australia

[a]Irina.Belova@newcastle.edu.au, [b]Graeme.Murch@newcastle.edu.au

Keywords: Interdiffusion, intrinsic diffusion, ionic conductivity, vacancy-wind effect, correlation factors.

Abstract. Net fluxes of vacancies commonly occur during chemical interdiffusion in alloys, ionic conductivity and the annealing out of radiation damage. When atoms with different jump rates diffuse in a net flux of vacancies the phenomenon of the vacancy-wind effect will occur. This effect, first discovered by the late Dr John Manning, is a subtle phenomenon arising from a disturbed distribution of vacancies with respect to a given moving atom or species of atom. In this paper, the vacancy-wind effect is discussed and its visualization, performed for the first time by computer simulation, is demonstrated.

Introduction

In the 1960s, the late Dr John Manning discovered the phenomenon of the vacancy-wind (sometimes also called the vacancy-flow) effect in solid state diffusion; see, for example [1,2] and references therein. Manning showed how the vacancy-wind effect is a natural result of a situation where there is a net flux of vacancies and two (or more) species of atom on the same lattice jump at different rates. A net flux of vacancies will normally occur in such situations as interdiffusion in binary and ternary etc alloys, d.c. ionic conductivity in ionic conductors and radiation damage annealing. In general terms, the vacancy-wind tends to make the more mobile atomic species somewhat slower than would be expected and the slower species somewhat faster than expected. In some rather extreme cases, Manning showed that even the direction of an atomic flux can be reversed because of the vacancy-wind. When it was first introduced, the vacancy-wind effect was somewhat controversial. It was probably not until 1979, when Monte Carlo computer simulation verified the phenomenon [3], that the vacancy-wind effect became universally accepted.

The vacancy-wind effect is intimately connected with the existence of non-zero off-diagonal phenomenological transport coefficients or L coefficients. In general, if the off-diagonal phenomenological coefficients are zero or are neglected (this is formally equivalent to the Darken approximation in interdiffusion [4]), then there is no vacancy-wind effect. The only known apparent exception to this statement is the case of diffusion by way of six-jump-cycles in intermetallic compounds [5]. It is worth mentioning that the terminology 'vacancy-wind' is actually somewhat of a misnomer since the general effect on the atomic fluxes can also occur as a result of atomic diffusion taking place via other defects such as dumb-bell interstitials in a net flux of such defects as might occur during radiation damage annealing.

The vacancy-wind effect is manifested as deviations in the 'expected' flow of *tracer* atoms in the driving force. In other words, given the tracer diffusion coefficients of the components (and the thermodynamic factor), the expected flow of those components in chemical interdiffusion can be predicted using Darken arguments [4]. These arguments permit the diagonal phenomenological coefficients to be related simply to the tracer diffusion coefficient (the off-diagonal phenomenological coefficients are ignored). When the actual flow of the components differs from

* This paper is dedicated to the memory of the late Dr John Manning.

this, then it can be ascribed to the vacancy-wind effect i.e. non-zero off-diagonal phenomenological coefficients.

The vacancy-wind effect is normally embodied *together with tracer correlation effects* in what are termed 'vacancy-wind factors'. These factors, of which quite a number have been presented in the solid state diffusion literature over the years, appear in various expressions relating collective transport quantities, such as interdiffusion coefficients and ionic conductivities, and the corresponding tracer diffusion coefficients of the components. Much of the initial understanding of the behaviour of vacancy-wind factors was provided by Manning himself using two well-known models: the five-frequency model and the random alloy model [1] and his own diffusion kinetics formalisms that were developed to describe diffusion in these models [1]. Since Manning's oeuvre, a more sophisticated and near exact theory to describe diffusion kinetics in the random alloy has been formulated [6]. This has necessitated a revisiting of the behaviour of the corresponding vacancy-wind factors [7].

Manning originally calculated the vacancy-wind factors in the same way as they occur, that is, in a driving force. As has been noted a number of times, Manning's arguments are rather difficult to follow. Furthermore, more recently, the vacancy-wind factors have invariably been calculated by assembly from the phenomenological coefficients themselves rather than in the way they occur i.e. in a driving force. Accordingly, visualization of the vacancy-wind effect is still missing, a fact that is plainly evident from a perusal of the available textbooks on solid state diffusion. The purpose of this paper is to present for the first time a visualization of the vacancy-wind effect using computer simulation. We will give examples using the random alloy model.

Vacancy-Wind Factors

In this section, we present expressions for the vacancy-wind factors as they appear in situations of ionic conductivity and chemical interdiffusion.

Vacancy-Wind Factors in Ionic Compounds (Two Conducting Ions). A vacancy-wind effect occurs in the d.c. ionic conductivity in systems where two or more ions (usually cations) share the same sublattice and compete for the same vacancies. Considering the partial d.c. ionic conductivities and assuming for convenience the same charge state q on each cation (A,B) we write that:

$$\sigma_A = \frac{C_A q^2 D_A^* p_A}{kT}; \qquad \sigma_B = \frac{C_B q^2 D_B^* p_B}{kT} \tag{1}$$

where the $p_{A(B)}$ are called partial vacancy-wind factors, C_A and C_B are the concentrations of the atomic components A and B, k and T are the Boltzmann constant and absolute temperature respectively and D^*_A and D^*_B are tracer diffusion coefficients for A and B respectively. These particular partial vacancy-wind factors have also been called "physical correlation factors" in the past, especially in the fast ion transport literature; see for example, [8]. The partial ionic conductivity vacancy-wind factors can be expressed exactly in terms of the tracer and collective correlation factors:

$$p_A = kT\frac{L_{AA}+L_{AB}}{C_A D_A^*} = p'_A\frac{1}{f_A}; \qquad p_B = kT\frac{L_{BB}+L_{AB}}{C_B D_B^*} = p'_B\frac{1}{f_B} \tag{2}$$

where we have introduced factors p'_A and p'_B for the purposes of considering the vacancy-wind effect itself that is wholly separate from the well-known tracer correlation effects. Indeed, it can be shown that p'_A and p'_B are equivalent to the partial vacancy correlation factors. Later in this paper, we will show how these factors can be physically understood in a vacancy flux using results of numerical simulations of diffusion under an applied electric field. The partial ionic conductivity vacancy-wind factors p_A and p_B give the deviation of the factors p'_A and p'_B from the

approximation of the partial vacancy correlations by tracer correlation factors f_A and f_B (correlated parts of the tracer diffusion coefficients).

When the Manning diffusion kinetics formalism for random mixing (the 'random alloy' model) is applied, we obtain the very simple result for p_A and p_B:

$$p_A = p_B = \frac{1}{f_0} \tag{3}$$

Or for p'_A and p'_B

$$p'_A = 1 - \frac{2c_B(D^*_A - D^*_B)}{M_0(c_A D^*_A + c_B D^*_B)}; \qquad p'_B = 1 + \frac{2c_A(D^*_A - D^*_B)}{M_0(c_A D^*_A + c_B D^*_B)} \tag{3a}$$

where M_0 is given by $M_0 = 2f_0/(1-f_0)$ and f_0 is the geometric tracer correlation factor. It is seen that the vacancy-wind effect in this situation of randomly mixed cations enhances the partial ionic conductivities of both cations equally and with a constant factor.

The partial ionic conductivities are very difficult to measure. On the other hand, the total ionic conductivity σ of the mixed system is straightforward to measure. The expression relating the total ionic conductivity to the individual tracer diffusion coefficients is:

$$\sigma = \sigma_A + \sigma_B = \frac{q^2}{kT} P\left(C_A D^*_A + C_B D^*_B\right) \tag{4}$$

where P is the total ionic conductivity vacancy-wind factor and q is the charge on the cations (assumed here for convenience to be the same). It is also worth noting that P (as presented in Eq. 4) has been used as a definition of (the reciprocal) of the Haven Ratio in mixed cation conductors such as glasses [9]. P can be expressed exactly in terms of the phenomenological coefficients (L_{ij}) and the tracer diffusion coefficients:

$$P = kT\frac{L_{AA} + L_{BB} + 2L_{AB}}{C_A D^*_A + C_B D^*_B} = P'\frac{c_A w_A + c_B w_B}{f_A c_A w_A + f_B c_B w_B} \tag{5}$$

where $w_{A(B)}$ are the atom-vacancy exchange frequencies for A(B) and $c_{A(B)}$ are the atomic compositions (site fractions) for A(B). Again we have introduced the factor P' to formally separate vacancy-wind effects from tracer correlation effects. P' is actually a total vacancy correlation factor and is a weighted average of the partial vacancy correlation factors [10].

Manning originally calculated the vacancy-wind factor P only for the five-frequency model [1]. P has been calculated for interacting systems for the purposes of modelling mixed solid state electrolytes [8]. As mentioned above, the random mixing (random 'alloy') model is also a useful model to employ here. Using the Manning diffusion kinetics formalism for the random alloy we find that the vacancy-wind factor P is simply equal to p_A and p_B and therefore:

$$P = \frac{1}{f_0} \tag{6}$$

Note that this result is only valid for the Manning diffusion kinetics formalism for the random alloy and in the very dilute vacancy limit where this theory is framed. When the very accurate MAA diffusion kinetics formalism for the random alloy is used to calculate P, the behaviour as shown in Fig. 1 is found, which is clearly quite different from the Manning result. However, when the vacancy-atom exchange frequencies are within about a factor of five, there is little difference between the results of Manning and MAA.

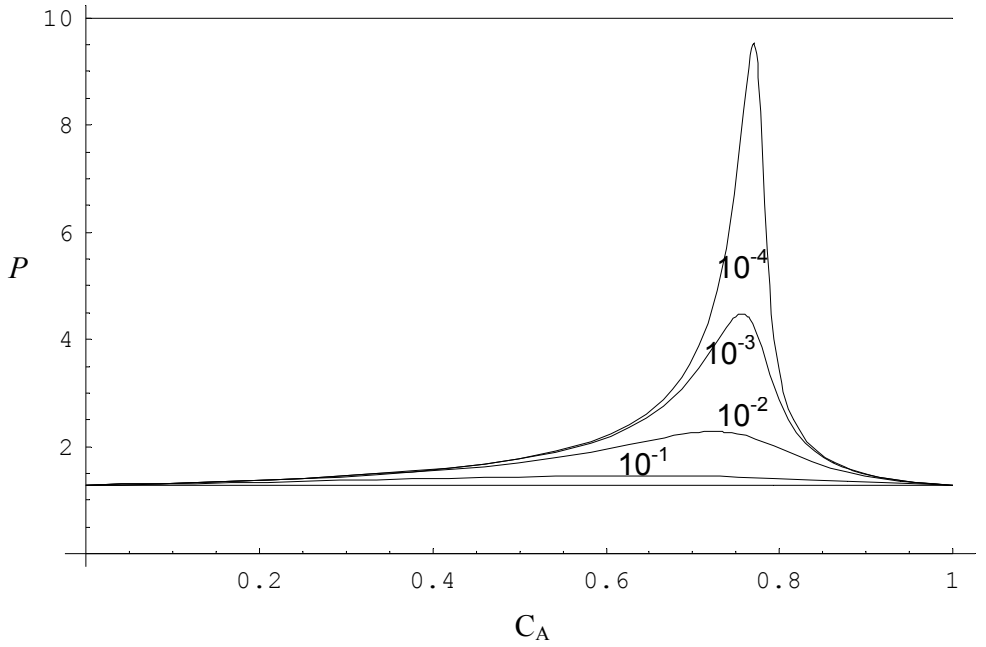

Figure 1. The vacancy-wind factor P in ionic conductivity (calculated using the MAA diffusion kinetics theory for the binary random alloy model) in the f.c.c. lattice as a function of composition c_A with $w_A/w_B = 10^{-1}, 10^{-2}, 10^{-3}, 10^{-4}$. (For the Manning approach P is $1/f_0$ i.e. 1.27967.)

The general strategy in revealing the physical nature of the vacancy-wind effect is to set up a moving reference frame(s) that moves with the atoms of interest. For example, for the ionic conduction case of an impurity moving with the host in a net flux of vacancies driven by the electric field the moving reference frame moves with the impurity itself. (For a species of atom we can focus on a given atom of that species.) In this moving reference frame the probability of finding a vacancy is determined at each site in a large region around the impurity or given atom. This is achieved by observing the present location of the vacancy with respect to that impurity or given atom at fixed time intervals (these are determined by using 'an attempt to jump' as the basic unit for the clock). These observations of the vacancy location are then readily averaged to obtain a map of the normalized probability of finding a vacancy as 'seen' by the moving impurity or given atom.

In Fig. 2 we show such a map of the normalized probability c_v*of finding a vacancy for the case where the impurity (A) has exactly the same vacancy-atom exchange frequency as the host (B) in a net flux of vacancies as driven by an electric field. Here, the vacancy flux J_V is from left to right (the atomic flux is from right to left). The impurity atom is shown as the solid square (■) in the figure. It can be seen that the map of the normalized probability of finding a vacancy is featureless, as of course it should be. There is no vacancy-wind effect here. The situation could be likened to a boat (the impurity) simply *drifting* in the current of a river (the host). There is no wave either at the bow or stern of the boat.

In Fig. 3 we show a map for the normalized probability of finding a vacancy for the case where the impurity has a higher vacancy-atom exchange frequency than the host in a net flux of vacancies as driven by an electric field. Again the vacancy flux is from left to right (the atomic flux is from right to left). The map of the normalized probability of finding a vacancy now has a large peak to the right of the impurity and a trough to the left. This means that the impurity now 'sees' a lower concentration of vacancies down-field and correspondingly higher concentration of vacancies up-field. Thus the drift of the fast-moving impurity in the field is diminished as a result of the vacancy-wind. The situation can be usefully likened to a boat (the impurity) that is going in the same direction as the river but is now also under power and is therefore moving faster than the current of the river. The bow wave (excess water) of the boat is equivalent to an excess of host atoms i.e. to a deficiency of vacancies. The trough (deficiency of water) at the stern of the boat is equivalent to a deficiency of host atoms i.e. to an excess of vacancies.

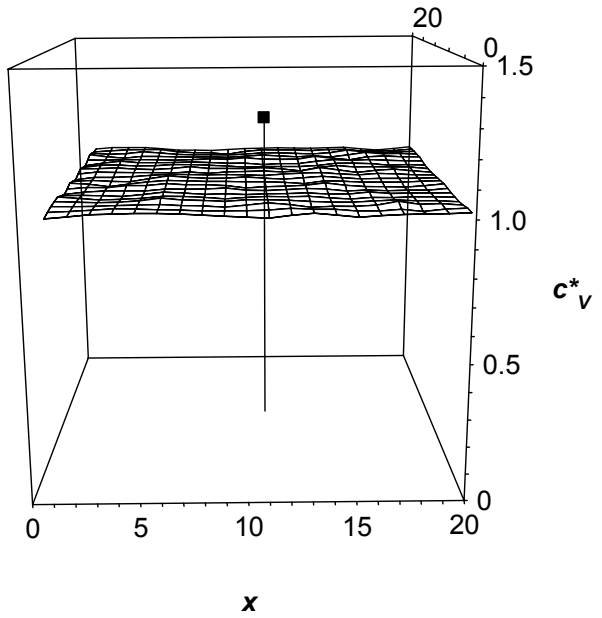

Figure 2. Visualization of the vacancy-wind effect for ionic conductivity. The normalized probability of finding a vacancy in the region around an impurity (A) in an electric field for the condition where $w_A=w_B$, $q_A=q_B$; f.c.c. lattice.

In Fig. 4 we show a map for the normalized probability of finding a vacancy for the case where the impurity now has a lower jump frequency than the host in a net flux of vacancies as driven by an electric field. Again the vacancy flux is from left to right (the atomic flux is from right to left). The map of the normalized probability of finding a vacancy now has a large trough to the right of the impurity and a peak to the left. This means that the impurity now 'sees' a higher concentration of vacancies down-field and a correspondingly lower concentration of vacancies up-field. Thus the drift of the slow moving impurity in the field is enhanced as a result of the vacancy-wind. The situation can be likened to a boat in a river that is going in the same direction as the river but is going slower than the river, e.g. it is now dragging its anchor. The build up of water at the stern of the boat i.e. the stern wave of the boat is equivalent to an excess of host atoms i.e. a deficiency of vacancies. The trough at the bow of the boat is equivalent to a deficiency of host atoms i.e. an excess of vacancies.

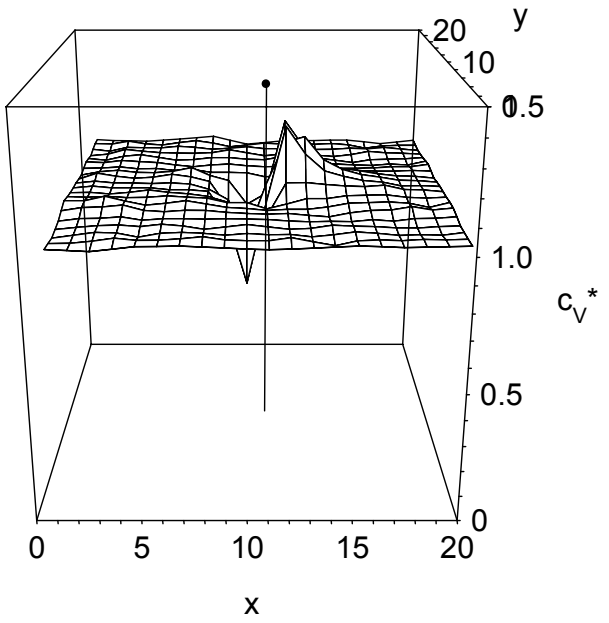

Figure 3. Visualization of the vacancy-wind effect for ionic conductivity. The normalized probability of finding a vacancy in the region around an impurity (A) in a host (B) in an electric field for the condition where $w_A=10w_B$, $q_A=q_B$; f.c.c. lattice.

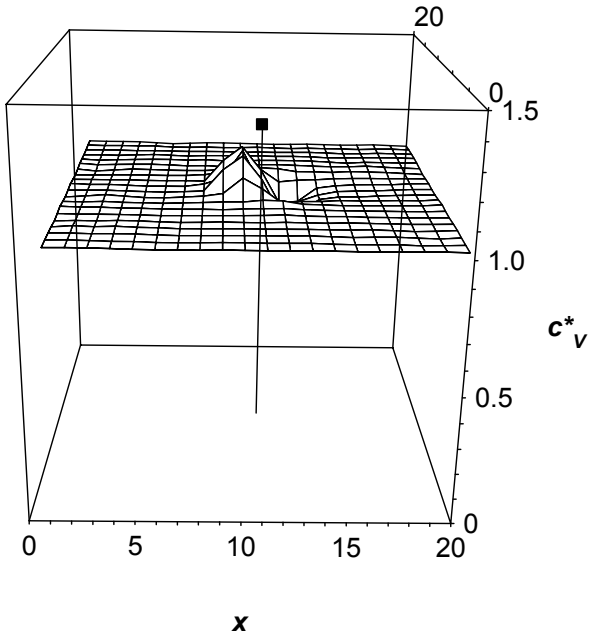

Figure 4. Visualization of the vacancy-wind effect for ionic conductivity. The normalized probability of finding a vacancy in the region around an impurity (A) in the host (B) in an electric field for the condition where $w_A = 0.1w_B$, $q_A = q_B$; f.c.c. lattice.

Interdiffusion in binary alloys. The vacancy-wind effect in diffusion in solids is almost certainly best known for the case of interdiffusion in binary alloys. In this situation, it is embodied in the vacancy-wind factor S appearing in what is usually called the Darken-Manning Equation. This important equation relates the interdiffusion coefficient, $\widetilde{D}$ to the two tracer diffusion coefficients D^*_A and D^*_B for the atomic components A and B respectively and the thermodynamic factor ϕ [1]:

$$\widetilde{D} = S(c_B D^*_A + c_A D^*_B)\phi \tag{7}$$

where c_A and c_B are the atomic compositions (site fractions) of A and B respectively and where the vacancy-wind factor for interdiffusion S is given exactly by:

$$S = kT\frac{c_B L_{AA}/c_A + c_A L_{BB}/c_B - 2L_{AB}}{C_B D_A^* + C_A D_B^*} = S'\frac{c_B w_A + c_A w_B}{f_A c_B w_A + f_B c_A w_B} \tag{8}$$

Here we have introduced the factor S' to separate tracer correlation effects. S' is a measure of the vacancy correlation that affects the atomic fluxes during interdiffusion in binary alloys. Then the vacancy-wind factor S can formally be described as the quantity which shows the deviation of the vacancy correlation contribution into the atomic flux from its approximation by tracer correlations. It should be pointed out that in the consideration of interdiffusion there is a physical assumption that the sources and sinks of vacancies are sufficiently numerous that vacancy under-saturation and super-saturation do not occur in the diffusion zone.

In the Darken approximation, the off-diagonal phenomenological coefficients are neglected and the diagonal phenomenological coefficients can be directly related to the tracer diffusion coefficients, i.e.

$$L_{ii} = c_i D^*_i/kT, \qquad L_{ij} = 0 \quad \text{for } i \neq j. \tag{9}$$

It is then seen from Eq. 8 that the Darken approximation puts $S = S' = 1$.

If we choose a particular model for the binary alloy, then expressions can then be developed for S in terms of measurable quantities, principally the tracer diffusion coefficients. For the binary random alloy model Manning was able to express the S factor in terms of the two tracer diffusion coefficients D^*_A, D^*_B and f_0, the geometric tracer correlation factor for the lattice (e.g. $f_0 = 0.78145$ for the f.c.c. lattice). Manning's expression is [1]:

$$S = 1 + \frac{2c_A c_B (D_A^* - D_B^*)^2}{M_0 (c_B D_A^* + c_A D_B^*)(c_A D_A^* + c_B D_B^*)} \tag{10}$$

or

$$S' = 1 - \frac{2[c_A c_B (D_A^* - D_B^*)^2 + f_0 D_A^* D_B^*]}{M_0 (c_A D_A^* + c_B D_B^*)^2} \tag{10a}$$

Although developed for the random alloy, it has been shown by Monte Carlo simulations that Eq. 7, with S given by Eq. 10, is surprisingly powerful. It provides quite a reasonable approximation even in intermetallic compounds of quite complex structures with the proviso that there is always a good deal of antistructural disorder; see, for example, [7].

Eq. 10 has become so closely identified with the Darken-Manning Equation that in some instances in the literature it has been implied that S is *always* given simply by Eq. 10. This is simply incorrect. Eq. 10 is purely a rather good approximation for S using Manning's diffusion kinetics analysis of the random alloy model. Eq. 10 gives for the limits of S: $1.0 \leq S \leq f_0^{-1}$. Accordingly, for the f.c.c. lattice (where f_0 is given by 0.78145), S is seen to take the upper limit of 1.27967.

The MAA theory [8], which has been developed since Manning's pioneering contributions, also describes diffusion kinetics in the random alloy model. The MAA formalism has been shown by recent extensive Monte Carlo simulation to provide an almost exact treatment for tracer correlation factors (the correlated parts of the tracer diffusion coefficients) and collective correlation factors (the correlated parts of the phenomenological coefficients) for the random alloy model and therefore all aspects of tracer and collective diffusion in the random alloy. In the case of the vacancy-wind factor S, an expression for S from the MAA formalism is unfortunately not available

in closed form and must be calculated numerically [9]. The MAA results for S are in good agreement with those of Manning for values of the atom-vacancy exchange frequency ratio within about a factor of five of unity. MAA gives unity as the lower limit for S (the same as the Manning approximation). However, instead of the Manning upper limit of f_0^{-1} as seen above, at compositions near the percolation threshold composition $c_A = f_0$, S approaches infinity when the ratio of the vacancy atom exchange frequencies w_A/w_B approaches zero, see Fig. 5. This finding has also been verified, where possible, by Monte Carlo simulation [7]. However, it should be noted that for practical purposes, even when the ratio of the vacancy-atom exchange frequencies of the two atomic components is as small as 1/100 (and this is probably quite rare in practice), S only increases to approximately two and then only at the percolation composition, see Figure 5.

To reveal the physical nature of the vacancy-wind effect for the interdiffusion in binary alloys we can perform an equivalent numerical simulation of the steady-state diffusion of atoms under applied electric forces with the special condition that $q_A = -c_B\, q_B/c_A$. We then again set up a moving reference frame(s) that moves with the atoms of interest. The observations of the vacancy location around this atom are then averaged to obtain a map of the normalized probability of finding a vacancy as 'seen' by the moving atom.

In Fig. 6 we show such a map of the normalized probability of finding a vacancy for the case of the binary alloy with $c_A = c_B = 0.5$ and $w_A = 10w_B$ in a net flux of vacancies as driven by an electric field. Fig. 6a is the map around a given A atom and Fig. 6b around a given B atom. Here, the vacancy flux J_V is again from left to right (the same for the flux of B atoms, but the flux of A atoms is from right to left). The atom of interest (A or B) is shown as the solid square in the figure. The map of the normalized probability of finding a vacancy now has a large peak to the right of the A atom and a trough to the left and vice versa for the B atom. This means that the atoms now 'see' a lower concentration of vacancies down-field and correspondingly higher concentration of vacancies up-field. Thus the drift of both types of atoms in the field is diminished as a result of the vacancy-wind.

In Figures 7 and 8 we show maps for the normalized probability of finding a vacancy for the case of the binary alloy with $c_A = 0.1$ (Figure 7) and $c_A = 0.01$ (Figure 8) and $w_A = 10\ w_B$ in a net flux of vacancies as driven by an electric field. Here, the vacancy flux J_V is again from left to right (the same for the flux of B atoms, but the flux of A atoms is from right to left). The atom of interest (A in Figure 7a and in Figure 8 is shown as a solid symbol, and B by an open symbol in Figure 7b). The map of the normalized probability of finding a vacancy again has an even larger (compared to the situation in Figure 6) peak to the right of the A atom and a trough to the left and vice versa for the B atom. This again means that the atoms now 'sees' a lower concentration of vacancies down-field and correspondingly higher concentration of vacancies up-field.

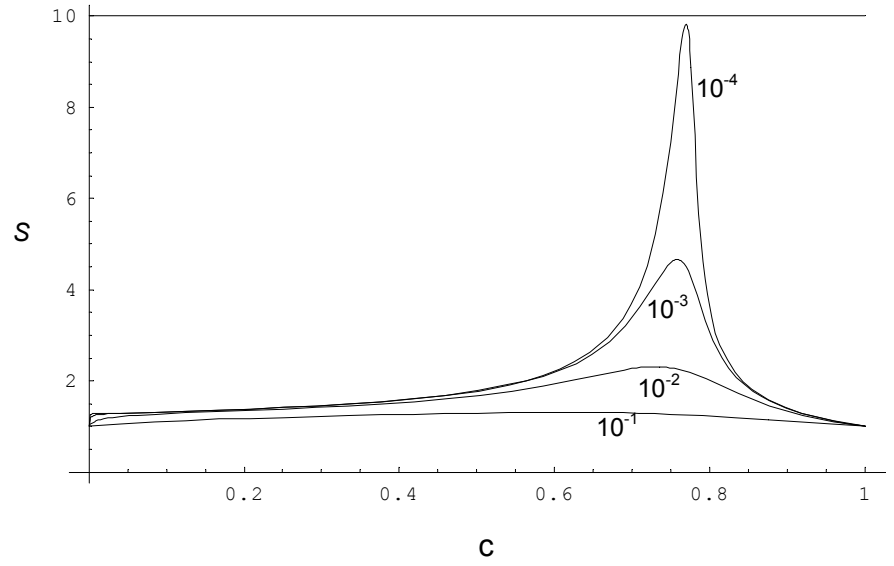

Figure 5. The vacancy-wind factor S in interdiffusion in a binary alloy (calculated using the MAA diffusion kinetics theory for the binary random alloy model) in the f.c.c. lattice as a function of composition c_A with $w_A/w_B = 10^{-1}, 10^{-2}, 10^{-3}, 10^{-4}$. (For the Manning approach the maximum value of S here is $1/f_0$ i.e. 1.27967.)

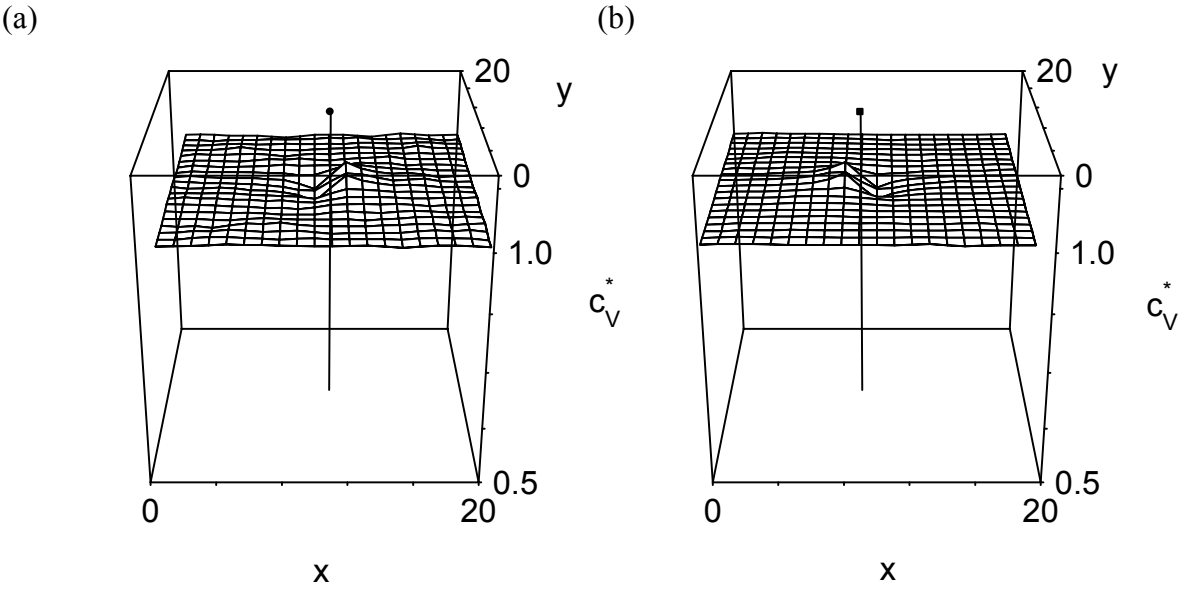

Fig 6. Visualization of the vacancy-wind effect for interdiffusion. The normalized probability of finding a vacancy in the region around an A atom see (a), and around a B atom see (b), for the composition $c_A = 0.5$ with the condition that $q_A = -c_B q_B / c_A$. Exchange frequencies are $w_A = 10\ w_B$.

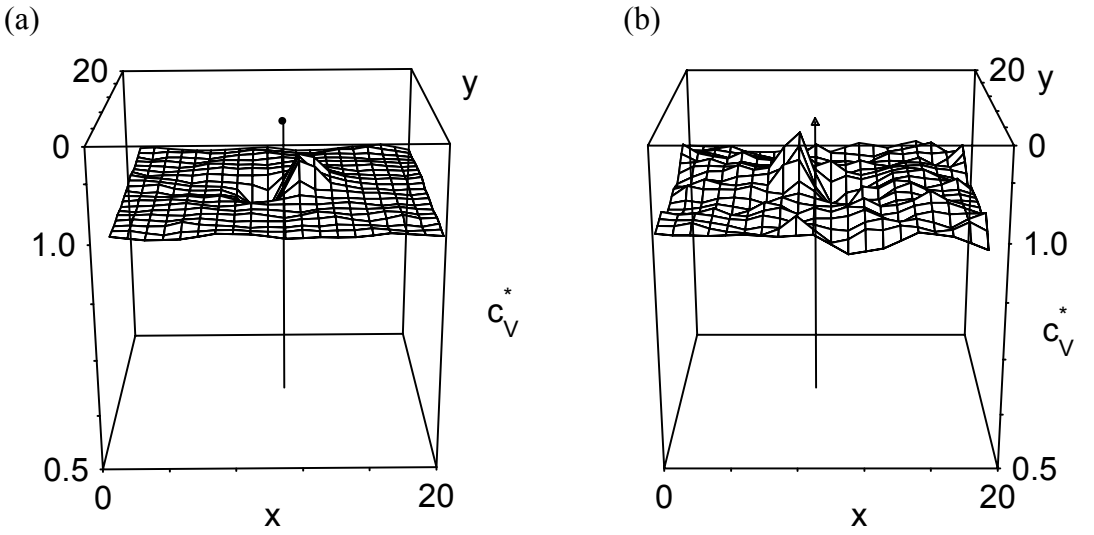

Figure 7. Visualization of the vacancy-wind effect for interdiffusion. The normalized probability of finding a vacancy in the region around an A atom see (a), and around a B atom see (b), for the composition $c_A = 0.1$ with the condition that $q_A = -c_B q_B / c_A$. Exchange frequencies are $w_A = 10 w_B$.

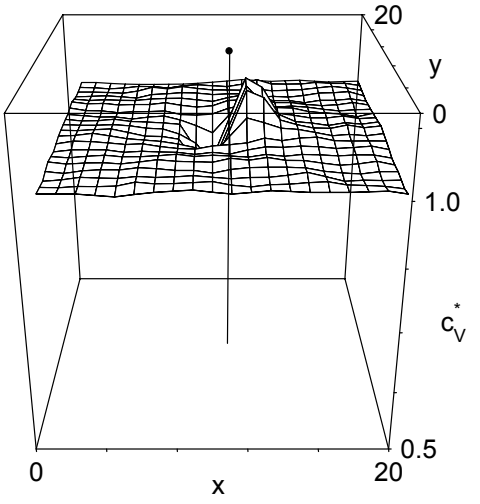

Figure 8. Vacancy-wind effect visualization for the interdiffusion coefficient for the composition $c_A = 0.01$ with the condition $q_A = -c_B q_B / c_A$ and $w_A = 10\ w_B$.

Apparent Vacancy-Wind Factors in Interdiffusion in Insulating Ionic Crystals. In cation interdiffusion in mixed-cation ionic crystals (with the cations having the same charge state) there are two limiting cases to consider. If there is abundant electronic conductivity then it is still appropriate to use the Darken-Manning Equation (Eq. 7) to relate the interdiffusion coefficient to the tracer diffusion coefficients (and the thermodynamic factor). On the other hand, if the ionic crystals are highly insulating and the mobility of the anions is very low compared with the cations (examples would be interdiffusion in some mixed silicates and carbonates with fixed valence cations), then the correct equation to use is what is popularly known in the solid state literature as the Nernst-Planck Equation, though strictly it is the Nernst-Hartley Equation:

$$\widetilde{D} = \frac{D_{A^*} D_{B^*}}{c_A D_{A^*} + c_B D_{B^*}} \phi \tag{14}$$

Interestingly, the Manning diffusion kinetics formalism for a random mixed system (the random alloy) is fully consistent with Eq. 14 as it stands. In other words, the Manning formalism gives no extra factor in Eq. 14 that might be considered as being analogous to a 'vacancy-wind factor'. However, when the near-exact MAA formalism for the random alloy is applied to the problem we do in fact find a non-trivial extra factor (that we have termed S^{NP}) that must be added to Eq. 14 [12], i.e.

$$\widetilde{D} = \frac{D_{A*}D_{B*}}{c_A D_{A*} + c_B D_{B*}} S^{NP}\phi \tag{15}$$

where the extra factor S^{NP} is described formally in terms of phenomenological coefficients and tracer diffusion coefficients by:

$$S^{NP} = kT\frac{L_{AA}L_{BB} - L_{AB}^2}{L_{AA} + L_{BB} + 2L_{AB}} \Big/ \left(\frac{Nc_A c_B D_{A*}D_{B*}}{c_A D_{A*} + c_B D_{B*}}\right) = S'_{NP}\frac{c_A w_A f_A + c_B w_B f_B}{(c_A w_A + c_B w_B) f_A f_B} \tag{16}$$

The Manning diffusion kinetics formalism has built into it relationships between the phenomenological coefficients and the tracer diffusion coefficients such that S^{NP} equals unity. Fig. 9 shows the behaviour of S^{NP} determined by the accurate MAA formalism for a range of ratios of the vacancy-atom exchange frequencies in the f.c.c. random alloy. In its formal presentation in Eq. 16, S^{NP} has the general appearance of a vacancy-wind factor. However, in interdiffusion of cations (of the same charge) of insulating ionic crystals with immobile anions there can clearly be no *net* cation vacancy flux. Nonetheless, as we will see below there are local vacancy fluxes for each species.

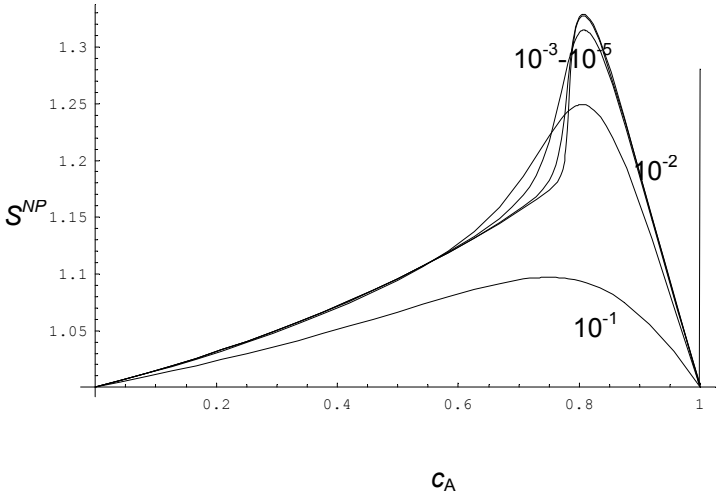

Figure 9. The factor S^{NP} (calculated using the MAA diffusion kinetics theory for the binary random mixing model) in the f.c.c. lattice as a function of composition c_A with $w_A/w_B = 10^{-1}$ - 10^{-5}. (For the Manning diffusion kinetics theory $S^{NP} = 1$.)

It is possible to visualize this apparent vacancy-wind effect in interdiffusion in insulating ionic crystals. In order to do so, we again perform steady-state in-field simulations in such a way as to simulate apparent interdiffusion in the mixed insulating ionic system at a particular composition. In order to achieve this, we 'tailor' the atomic charges q_A and q_B, in such a way that they obey the following relation (note that we are able to do visual simulations for the vacancy-wind effect only for a constant composition):

$$q_A = -\frac{L_{BB} + L_{AB}}{L_{AA} + L_{AB}} q_B \tag{17}$$

Then, in the simulation, we have for the fluxes of the A and B atoms:

$$J_A^0 = c_A w_A S'_{NPA} q_A E = \frac{L_{AA}L_{BB} - L_{AB}^2}{(L_{BB} + L_{AB})\beta} q_A E$$

$$J_B^0 = c_B w_B S'_{NPB} q_B E = \frac{L_{AA}L_{BB} - L_{AB}^2}{(L_{AA} + L_{AB})\beta} q_B E \tag{18}$$

It is easy to show that the corresponding actual S'_{NP} (see above in Eq. 16) will be a weighted geometric average of the S'_{NPA} and S'_{NPB} that can be generated in the simulation (see Figure 10):

$$(S'_{NP})^{-1} = [(S'_{NPA} c_A w_A)^{-1} + (S'_{NPB} c_B w_B)^{-1}][(c_A w_A)^{-1} + (c_B w_B)^{-1}] \tag{19}$$

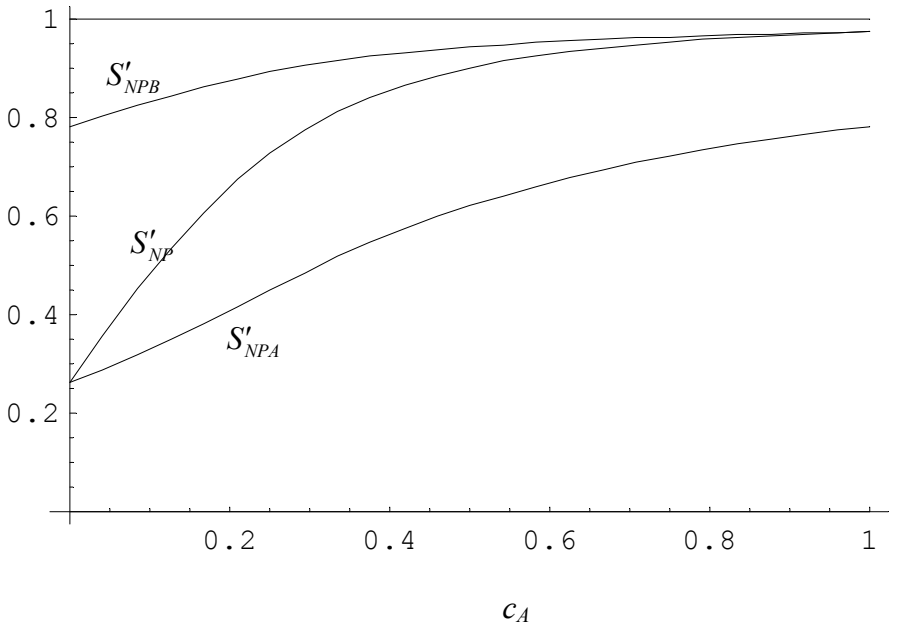

Figure 10. Vacancy-wind factors S'_{NP} (Eq 17), S'_{NPA} and S'_{NPB} (Eqs. 18) for the case of $w_A = 10\ w_B$. All vacancy-wind factors calculated according to MAA.

In Figure 11a,b we present S'_{NPA} and S'_{NPB} for the case when $c_A = 0.5$ with $w_A = 10\ w_B$. Similarly, in Figure 12a,b we present S'_{NPA} and S'_{NPB} for the case where $c_A = 0.1$ with $w_A = 10\ w_B$. In these figures, the A atoms drift from right to left and the B atoms drift from left to right. The net vacancy flux is zero. But each of the atomic fluxes clearly generates a non-zero partial vacancy flux. It can be seen that in this situation *both* A and B atoms simultaneously 'see' local vacancy fluxes and, particularly, a lower probability of vacancies in their respective drift directions. This results in a diminishment of the drifts of both species.

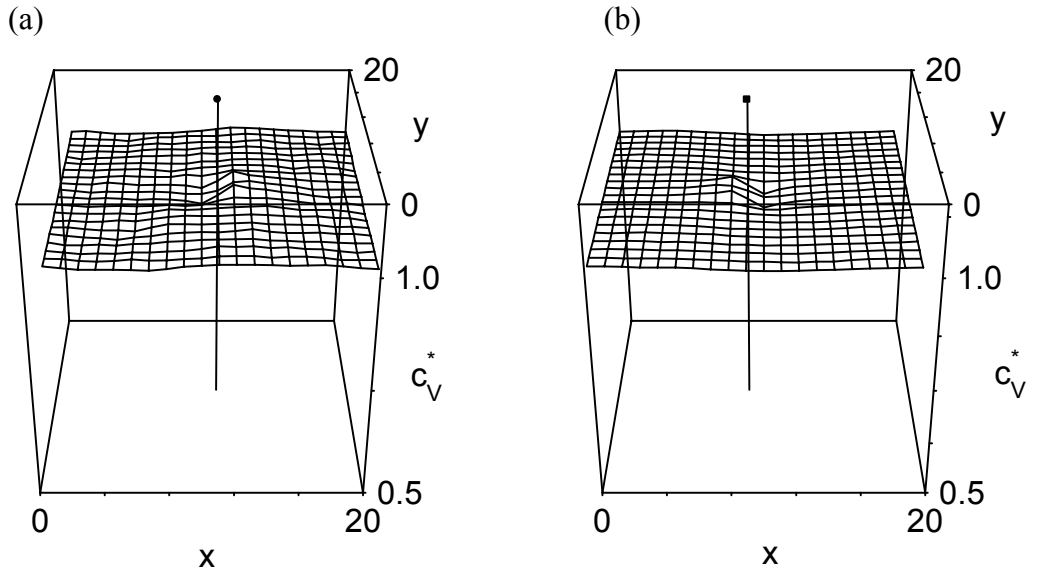

Figure 11. Vacancy-wind effect visualization for the interdiffusion in insulating ionic crystals for the composition $c_A = 0.5$ with the condition $q_A = -(L_{BB} + L_{AB})q_B/(L_{AA} + L_{AB})$ and $w_A = 10\ w_B$. a): S'_{NPA} and b): S'_{NPB}.

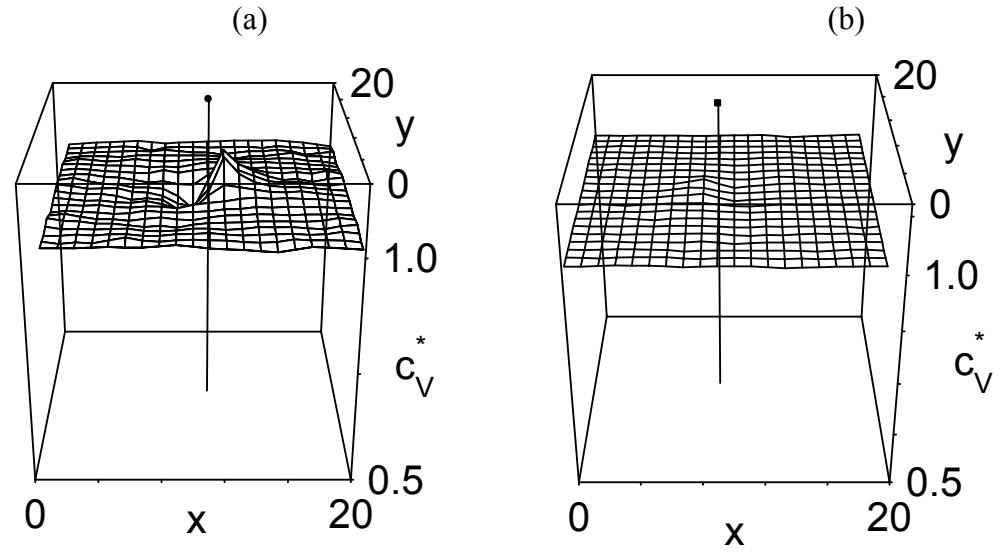

Figure 12. Vacancy-wind effect visualization for the interdiffusion in insulating ionic crystals for the composition $c_A = 0.1$ with the condition $q_A = -(L_{BB} + L_{AB})q_B/(L_{AA} + L_{AB})$ and $w_A = 10\ w_B$. a): S'_{NPA} and b): S'_{NPB}.

We can see that the results for the vacancy correlation effects are similar in magnitude to the previous cases. Nonetheless, since the reference condition refers to tracer diffusion coefficients (which obviously contain tracer correlation effects which are strong) the net result on the vacancy-wind factor S^{NP} itself is an enhancement. But here, this factor is considerably smaller than in the previously considered cases of vacancy-wind effects in ionic compounds and in interdiffusion in binary alloys.

Conclusions

Net fluxes of vacancies commonly occur during chemical interdiffusion in alloys, ionic conductivity and the annealing out of radiation damage. When atoms with different jump rates diffuse in a net flux of vacancies the phenomenon of the vacancy-wind effect occurs. This effect, first discovered by the late Dr John Manning, is a subtle phenomenon arising from a disturbed

distribution of vacancies with respect to a given moving atom or species of atom. In this paper, the vacancy-wind effect was discussed and its visualization, performed for the first time by computer simulation, was demonstrated for vacancy-winds occurring in ionic conductivity, interdiffusion in binary alloys and interdiffusion in mixed insulating ionic crystals. The model used for the visualization was the random alloy model.

Acknowledgement

This research was supported by the Australian Research Council.

References

[1] J.R. Manning: *Diffusion Kinetics for Atoms in Crystals* (Princeton, NJ: Van Nostrand) 1968.
[2] J.R. Manning: Phys. Rev. B Vol. 4 (1971), p. 1111.
[3] G.E. Murch and R.J. Thorn: Phil. Mag. A Vol. 39 (1979), p. 259.
[4] L.S. Darken: Trans. AIME Vol. 180 (1948), p. 430.
[5] G.E. Murch and I.V. Belova: Phil. Mag. A Vol. 81 (2001), p. 83.
[6] A.R. Allnatt and E.L. Allnatt: Phil. Mag. A Vol. 49, (1984), p. 625.
[7] I.V. Belova and G.E. Murch: Defect Diffus. Forum Vols. 237-240 (2005), p. 291.
[8] L.K. Moleko, A.R. Allnatt and E.L. Allnatt: Phil. Mag. A Vol. 59 (1989), p. 141.
[9] I.V. Belova and G.E. Murch: Phil. Mag. A Vol. 81 (2001), p. 1749.
[10] I.V. Belova and G.E. Murch: Acta Mat. Vol. 55 (2007), p. 627.
[11] S.V. Divinski, F. Hisker, Chr. Herzig, R. Filipek, M. Danieleweski: Defect Diffus. Forum Vols 237-240 (2005), p. 50.
[12] A. Suzuki, H. Sato and R. Kikuchi: Phys. Rev. B Vol. 29 (1984), p. 3550.
]14] A.W. Imre, S. Voss and H. Mehrer: J. Non-Cryst. Solids Vol. 333 (2004), p. 231.
[15] I.V. Belova A.R. Allnatt and G.E. Murch, Phil. Mag. accepted for publication and in press.